

# Design and Fabrication of a Foldable Hexapod Robot Towards Experimental Swarm Applications

Mahdi Agheli, Siamak G. Faal, Fuchen Chen, Huibin Gong, and Cagdas D. Onal

**Abstract**—This paper presents the development of a lightweight origami-inspired foldable hexapod robot. Using a single sheet of polyester and a laser cutter, the hexapod robot can be fabricated and assembled in less than one hour from scratch. No screw or other external tools are required for assembly. The robot has built-in polyester fasteners considered in its crease pattern. The design uses four-bar mechanisms, which makes the robot flexible to be adjusted for different speeds or other task metrics. For a given desired locomotion velocity, various parameters of the four-bar mechanisms in the crease pattern can be modified accordingly. Design flexibility, ease of fabrication, and low cost make the robot suitable as an agent for swarm objectives. This work presents the foldable hexapod design and its kinematic analysis. The robot is fabricated, assembled, and tested for functionality. Experimental results show that the robot prototype runs with a maximum forward speed of 5 body lengths per second and turns in place with a speed of 1 revolution per second. The final robot weighs 42 grams.

## I. INTRODUCTION

The collective behavior of a dense group of objects moving in large numbers is usually known as a swarm. Ants or bees are examples of swarm in nature. The development of a bio-inspired robotic swarm of ground robots is the main motivation of this work, where the overall task will be robust to operational failures of members. While agents can be relatively simpler in a multi-robot setting, they still need to satisfy low-level objectives such as locomotion and steering on unstructured or rough terrain. This paper addresses the design and fabrication of a mobile robot by folding a single sheet of plastic based on origami concepts, capable of maneuvering on rough terrain and suitable for rapid and inexpensive production towards experimental many-robot applications.

Legged robots offer a salient solution for maneuvering on rough terrain. More specifically, the hexapod mechanism attracts attention due to its similarity to a variety of insects and ability to negotiate unstructured terrain with a high level of stability [1], [2], [3], [4], [5], [6]. In addition to maneuverability, high-speed, low-cost, and straightforward fabrication and operation of mobile robot agents plays a significant role for experimental many-robot systems of the future. Hexapod robots such as those presented in [7], [5], [6] that require considerable alignment and assembly operations of many distinct parts are not optimal for these

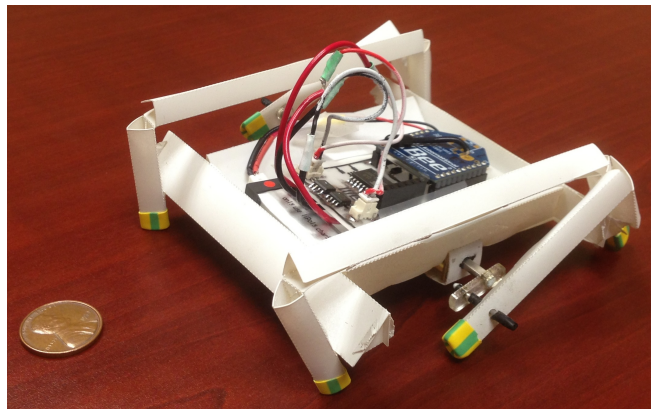


Fig. 1. Printed and folded hexapod mobile robot prototype.

applications. Promising results that utilize minimal Degrees of Freedom (DOF) include DASH [8] and Kilobot [9]. DASH is a lightweight and fast hexapod robot that is suitable for locomotion on unstructured terrain. It utilizes the Smart Composite Microstructure (SCM) process for fabrication, which requires multi-layer alignment and a number of parts that need to be assembled. On the other hand Kilobot is a low-cost system developed for tabletop experimental multi-robot studies that are not suitable for real environments.

Our objective in this research is to fill the gap between robots like Kilobot and DASH by making a robot with high maneuverability as well as easy and cost-effective fabrication process. Here, we propose a new design of a hexapod robot to satisfy these requirements while it is able to walk in rough environment. For this purpose, we take advantage of origami technique. It has been shown that origami, the traditional Japanese art of paper folding, is a reliable technique for fabricating robots by folding planar sheets. Felton et.al [10], [11] used origami for self-folding of shape memory composite, and Onal et.al showed an origami-inspired approach to make worm robots [12].

In this paper, we use the same origami technique to make our hexapod robot. Our robot is “printed” by laser machining a single polyester sheet [7] and then folded. Our printed and folded hexapod robot is shown in Fig. 1. The presented design in this paper does not use any external fasteners. All fasteners are embedded in the crease pattern, which reduces the assembly time. The robot is folded from a single sheet of plastic. The presented hexapod in this paper uses only two DC motors, the minimum number of actuators required for 2-D maneuverability with a differential drive controller. The electronic control circuitry is custom fabricated as part of

Mahdi Agheli, Huibin Gong, and Cagdas D. Onal are with the Mechanical Engineering Department, Worcester Polytechnic Institute, MA 01609, USA {mmagheli, hgong, cdonal}@wpi.edu

Siamak G. Faal and Fuchen Chen are with the Robotic Engineering Program, Worcester Polytechnic Institute, MA 01609, USA {sghorbanifaal, fchen}@wpi.edu

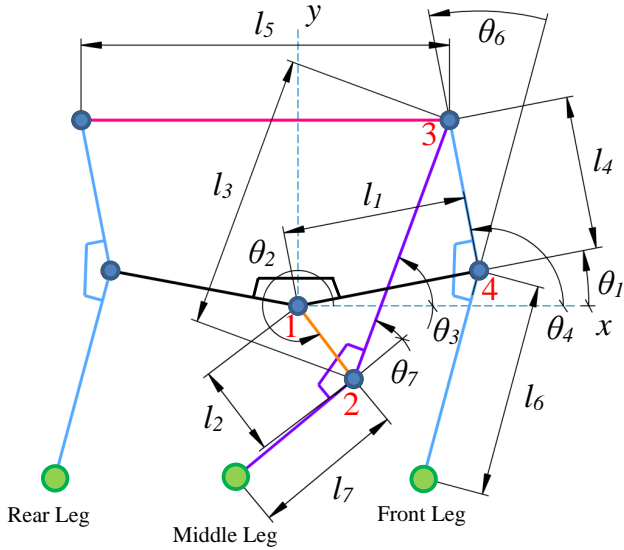


Fig. 2. The generalized four-bar leg mechanism considered in the design of our foldable hexapod robot.

the robot manufacturing process and embedded on the robot body, which reduces the cost compared to using commercial circuits. The presented hexapod weighs 42 g and is designed to run based on the tripod gait as the fastest walking gait.

## II. CONCEPTUAL DESIGN

In this section, the design considerations and requirements of a hexapod robot for the proposed swarm application has been explained. The discussion is followed by the details of the conceptual design, which satisfies the required design constraints.

### A. Design Considerations

Hexapod robots have been used commonly because of their innate balance and locomotion capability. To have enough versatility and maneuverability over highly cluttered terrain, the robot needs to have at least 18 active DOF, three per leg, in its joint space. Having 18 actuators dramatically increases the cost, weight, and size of the robot. This makes an 18-DOF robot an inefficient agent for swarm applications. A possible solution is to reduce the cost of each robot by reducing the number of actuators. However, reducing the number of active DOF of the robot will reduce its maneuverability and workspace. For our swarm objective, the robot needs to have capability to walk, turn, and maneuver over rough terrain. To satisfy this need, a minimum of two actuators is required, one for each side of the robot body. This configuration will allow the hexapod robot to benefit from a differential drive locomotion system.

The other design requirement is to keep the weight of the robot as low as possible. While reducing the number of the actuators will reduce the weight of the robot, it is possible to further reduce the weight by using a lightweight material. The material used should be invulnerable to collisions. To satisfy this need, the main body of the robot is formed by

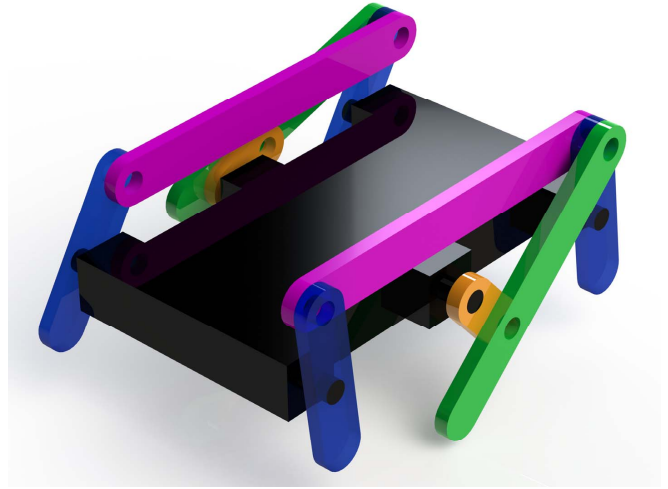


Fig. 3. The proposed design of a 2-DOF hexapod mobile robot.

folding a polyester sheet. Since the manufacturing process includes only laser cutting and folding the polyester, the manufacturing cost is minimal.

### B. Proposed Design

The designed robot is conducted by a main body to which two extended four-bar mechanisms are attached. The robot is considered to be longitudinally symmetric and it is designed to walk based on tripod gait.

Let's define legs of the robot as follows: Front Left (FL), Middle Left (ML), Rear Left (RL), Front Right (FR), Middle Right (MR), and Rear Right (RR). All three left legs (FL, ML, and RL) are part of the same mechanism which is achieved by extending a single four-bar as will be discussed later. In the same way, all three right legs (FR, MR, and RR) are part of another four-bar mechanism with the same design as the left one. When the left four-bar mechanism works, legs FL and RL have 180-degree phase difference with the leg ML. On the other side of the robot, legs FR and RR have 180 degrees phase difference with the leg MR. All we need to do to have a tripod gait is to keep a 180-degree phase difference between the left and right four-bar mechanisms. In this way legs FL, MR, and RL will be in the same phase, and legs FR, ML, and RR will be in the same phase as well but with 180 degrees phase difference with the other legs. This enables the robot to walk using a tripod gait, which is the fastest locomotion gait possible for a hexapod mobile robot. The design and parameters are shown in Fig. 2 and Fig. 3. As shown, Fig. 3 is a simplified version of its general design depicted in Fig. 2. However, the presented analysis will retain its generality.

As shown in Fig. 2, the design starts with a simple four-bar mechanism 1-2-3-4 with the grounded link of 1-4. The link 3-4 is then extended to create the front leg and the link 2-3 is extended to create the middle leg. For the rear leg, as we discussed, we need it to be in the same phase as the front leg. Therefore, a parallelogram is created to achieve this goal. The exact same mechanism is designed for the other

side of the robot.

### III. KINEMATIC ANALYSIS AND DESIGN OPTIMIZATION

Our final design for the four-bar based hexapod mobile robot is developed as a result of an optimization process to maximize the running speed of the robot.

#### A. Full Kinematic Analysis

As shown in Fig. 2, the kinematics of the mechanism used for each side of the robot is governed by the central crank-rocker mechanism as depicted in Fig. 3. The analysis of this four-bar mechanism is required for the robot's locomotion analysis and gait optimization.

We refer to  $c_i$  and  $s_i$  as the cosine and sine of angle  $\theta_i$ , respectively. Writing vector loops along  $x$  and  $y$  axes, yields the position equations:

$$l_2c_2 + l_3c_3 - l_4c_4 - l_1c_1 = 0, \quad (1)$$

$$l_2s_2 + l_3s_3 - l_4s_4 - l_1s_1 = 0. \quad (2)$$

Solving (1) and (2) for  $\theta_3$  and  $\theta_4$  using the method introduced in [13] results in:

$$\theta_3 = \text{atan2}(b, a) \pm \text{atan2}\left(\sqrt{a^2 + b^2 - c^2}, c\right), \quad (3)$$

$$\theta_4 = \text{atan2}(R_y + l_3s_3, R_x + l_3c_3), \quad (4)$$

where  $R_x$ ,  $R_y$ ,  $a$ ,  $b$ , and  $c$  are defined as:

$$R_x = l_2c_2 - l_1c_1, \quad (5)$$

$$R_y = l_2s_2 - l_1s_1, \quad (6)$$

$$a = 2l_3R_x, \quad (7)$$

$$b = 2l_3R_y, \quad (8)$$

$$c = l_4^2 - R_x^2 - R_y^2 - l_3^2. \quad (9)$$

In the above equations,  $l_i$  represents the length of the link  $i$  illustrated in Fig. 2. As can be seen in (3), there are two solutions for the value of  $\theta_3$  for any value of  $\theta_2$ . These two solutions correspond to the open and crossed configurations of the mechanism. In our design, we have used the crossed configuration.

*Velocity:* To obtain the angular velocities, one can directly differentiate (1) and (2) as follows:

$$-l_2\dot{\theta}_2s_2 - l_3\dot{\theta}_3s_3 + l_4\dot{\theta}_4s_4 = 0, \quad (10)$$

$$l_2\dot{\theta}_2c_2 + l_3\dot{\theta}_3c_3 - l_4\dot{\theta}_4c_4 = 0. \quad (11)$$

Solving (10) and (11) for  $\dot{\theta}_3$  and  $\dot{\theta}_4$  yields:

$$\dot{\theta}_3 = -\frac{l_2\dot{\theta}_2s_2s_4}{l_3s_3s_4}, \quad (12)$$

$$\dot{\theta}_4 = -\frac{l_2\dot{\theta}_2s_2s_3}{l_4s_3s_4}, \quad (13)$$

where  $s_{ij} = \sin(\theta_i - \theta_j)$ .

Using (3), (4), (12), and (13), it is possible to compute the position and velocity of all the points on the mechanism.

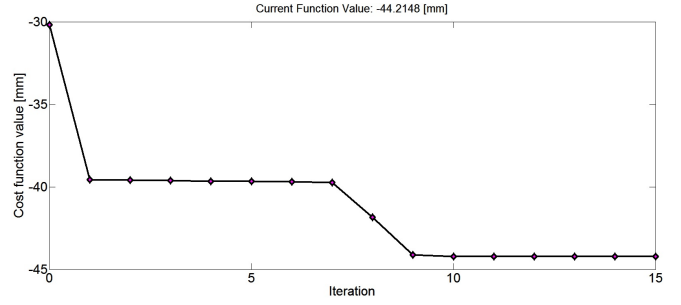


Fig. 4. Cost function values during the kinematic design optimization process.

#### B. Design Optimization

In order to correct the gait sequence of the robot, the proposed mechanism needs to be optimized. The main objective of the optimization is to minimize the vibrations introduced to the motion of the robot, by correcting the direction of the velocity vectors of the active feet. The active feet are defined as the link tips that are in contact with the ground. A perfect gait sequence is achievable by having all the velocities of the active feet in the same direction and parallel to the body of the robot. However, imposing this constraint on the optimization algorithm results in an empty feasible space. This conclusion has been made by running the optimization algorithm from five-hundred different random initial points. In order to bypass this problem, the objective function is chosen to maximize distance traveled along the body of the robot by the active feet. The details of the optimization formulation are presented in what follows.

*Design variables:*

$l_1$ ,  $l_3$ , and  $l_4$

*Constant values:*

$l_2 = 20\text{mm}$

$l_6 = l_7 = 15\text{mm}$

$\theta_6 = \theta_7 = 0\text{rad}$

$l_{min} = 5\text{mm}$  : minimum feasible length of the links

$l_{max} = 70\text{mm}$  : maximum feasible length of the links

*Dependent variables:*

$l_5 = 2l_1$

*Constraints:*

$g_1$  to  $g_3$ :  $l_{min} \leq l_i \leq l_{max}, \forall i \in \{1, 3, 4\}$

$g_4$  to  $g_6$ :  $l_2 - l_i + \varepsilon \leq 0, \forall i \in \{1, 3, 4\}$

$g_7$ :  $l_2 + S - \sum l_i + \varepsilon \leq 0$  for  $S = \max\{l_1, l_3, l_4\}$  and

$i \in \{1, 3, 4\} - \{i_S\}$

$g_8$ :  $\pi/6 \leq \theta_4 \leq 5\pi/6$

*Objective function:*

$Cost = -\int v_{ma} \cdot e_x dt - \int v_{fa} \cdot e_x dt,$

where  $v_{ma} \cdot e_x$  and  $v_{fa} \cdot e_x$  are the velocities of the middle and front active feet of the robot along the  $x$  axis, which is

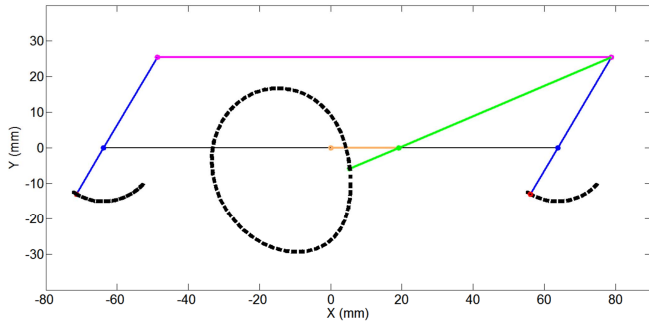


Fig. 5. Foot trajectories of the hexapod robot as a result of the velocity-based kinematic design optimization.

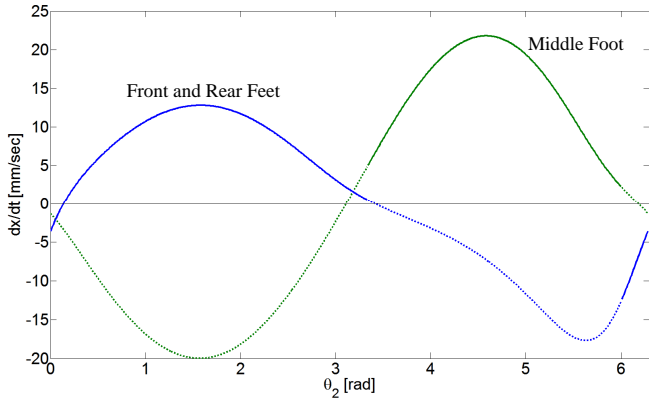


Fig. 6. Velocity patterns of the front, rear, and middle feet of the hexapod robot as a result of kinematic design optimization.

parallel to the body of the robot. The constraints  $g_1$ ,  $g_2$ ,  $g_3$ , and  $g_8$  deal with the feasibility of the design using the folding technique which is discussed in Section IV. Constraints  $g_4$  to  $g_6$  are forcing  $l_2$  to remain as the crank of the mechanism. Finally, the constraint  $g_7$  deals with the Grashof condition. Since implementation of an optimization problem solver is beyond the scope of this paper, available software packages are used to solve this problem.

In this regard, two different optimization algorithms available in MATLAB software are considered: the gradient based and genetic algorithm based optimization methods. Since the system is highly nonlinear, it is obvious that the values obtained for the design variables might not be the global optimal solution of the system. To address this issue, the optimization code is evaluated from different initial values and the solution that yields the minimum cost function is chosen as the final solution of the system. The minimization of the cost function and the final cost value are depicted in Fig. 4.

The trajectories of each foot of the robot are illustrated in Fig. 5. The velocities of the middle and front feet of the robot along the x-direction as functions of  $\theta_2$  are illustrated in Fig. 6. Solid and dotted lines represent the status of each feet. While the velocity of the active foot is depicted with solid lines, the velocity of the inactive foot is depicted with dotted lines. In this figure, the blue curve illustrates

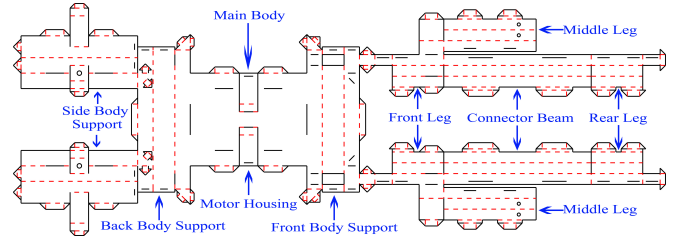


Fig. 7. The crease pattern of the foldable hexapod robot. Specific part of interest are marked. Black solid lines indicate cuts and red dashed lines indicate folds.

the velocity of the front and rear feet and the velocity of the middle foot is illustrated by green color. As discussed before, since there are no constraints on the direction of the velocities, there are some instances that the active foot has a velocity in the opposite direction of the robots movement (i.e. negative velocities in the case of Fig. 6). Although the lack of constraints on the velocities of each feet will introduce vibrations on the movement of the robot, the overall movement in a specific direction is guaranteed with the chosen objective function. As depicted in Fig. 6, the total integral of the active feet is considerably larger than zero which will cause a net displacement in the forward direction.

#### IV. FABRICATION AND EXPERIMENTAL RESULTS

As shown in Fig. 7, our robot is made out of one single sheet of plastic. The black lines in the crease pattern need to be cut and red dashed lines are folding lines.

At the beginning, a side view of the hexapod is drawn for reference. From the picture shown, a rectangle piece of plastic with triangular beam on every side is used as the base of the robot, which provides rigidity and stability. Six legs of the robot are also triangular beams of 7 mm on each side. Between two legs, we cut through only two sides of the triangle and the uncut side keeps them connected. Such mechanism provides a one degree of freedom flexure joint and thus acts as the connector between legs. Then the linkage system we designed in the previous section can be realized.

We also develop a method to lock folded plastic together because the plastic tends to return to its original shape after being folded. Such a self-locking mechanism is achieved by first adding a trapezoid-shape key and a hole on the corresponding place where we want to fix the item on. Then, following the crease pattern on the key, we can fold it into a rectangle which can go through the hole. After that, we then unfold the key to prevent it from coming off. After many experiments, this method proves to be the most reliable and force the folded plastic to stay in the desired shape.

The key and hole design not only allows us to avoid using screws and nuts, but also leads to another design principle to help us mount the motor and other potential discrete electromechanical components on the robot using the plastic as a holder. Three rectangles are folded into a box while one of the rectangles has a hole in the middle. The motor then is inserted in the box while the crank goes through the hole.

This way, the motor is permanently mounted in its desired position and the main body wont rotate.

Laser machining the entire crease pattern takes approximately 5-6 minutes depending on the speed of the laser cutter. When finished, the crease pattern becomes its own blueprint such that almost everyone can follow the crease pattern and fold the hexapod. On average, an experienced researcher can build the hexapod within an hour. After folding several robots, we find that sometimes it is relatively difficult to insert a small key in to the hole, so we try to add a small triangle on the shorter side of the trapezoid which greatly reduces the difficulty of locking.

The main controller of the robot uses ATMEL ATtiny2313 microcontroller to control the applied voltage to the two Permanent Magnet Brushed DC (PMBDC) motors that run the cranks on the left and right side mechanisms. To do so, The Pulse Width Modulation (PWM) signals generated by microcontroller are fed into two H-bridges that are connected to the terminals of the PMBDC motors. An Xbee module is used to send wireless commands to the robot using asynchronous serial communication. With the use of a small lithium polymer battery (3.7 V, 160 mAh, 4 g) as the main power source of the robot. The custom made Printed Circuit Board (PCB) of the controller is etched using a simple solid ink printer and an etching tank that contains Ferric Chloride solvent. Although, for this prototype, the circuit is etched from a separate plastic sheet laminated with copper, the etching technique provides a unique method of creating the circuit on the same sheet that forms the body of the robot.

The overall robot manufacturing time from scratch is around, but less than an hour. The fabricated robot has a ground clearance of 15 mm. A rubber cover is used on the feet to provide extra friction during motion. We tested our foldable hexapod robot prototype to validate its kinematic functionality. We ran the robot many times in different directions over various surfaces.

The robot achieved a maximum forward running velocity of 5 body lengths per second. The speed of the robot was observed to be fluctuating between this maximum value and lower speeds. From inspection, the reason was found to be in variations in the phase difference between the leg mechanisms on both sides. As mentioned before, maximum locomotion speed can only be achieved when the two four-bar mechanisms operate in opposite phase. In this case, the robot runs based on the tripod gait with full speed. However, because of errors in the gear motors driving the mechanisms, this phase difference was not fixed. The fluctuation in the motors varied the amount of phase difference between zero and 180 degrees. Therefore, the average speed of the robot can be considerably improved if the phase difference can be controlled or kept constant at 180 degrees. Fig. 8 shows snapshots of the robot during a forward locomotion experiment over a linear displacement of 1 body length.

Due to its differential steering mechanism, our foldable hexapod prototype can achieve very tight turns. By running the two four-bar mechanisms in opposite directions the robot can readily turn in place. The in-place turning velocity of the

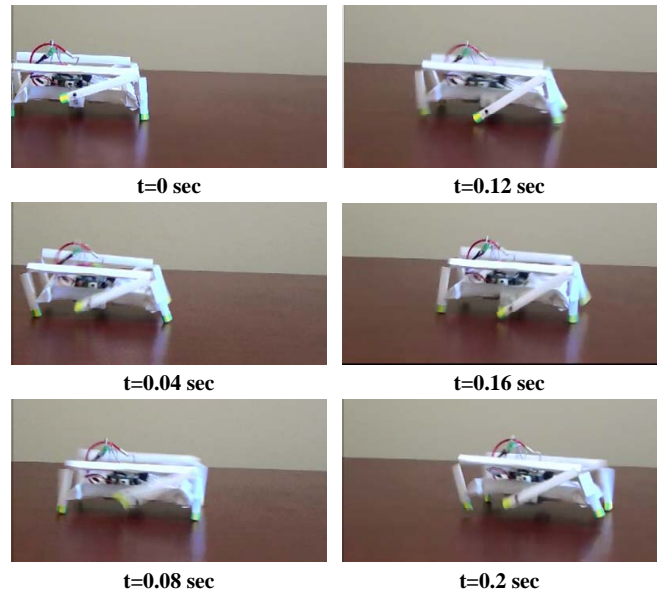


Fig. 8. Snapshots of the foldable hexapod robot prototype during a linear forward locomotion experiment.

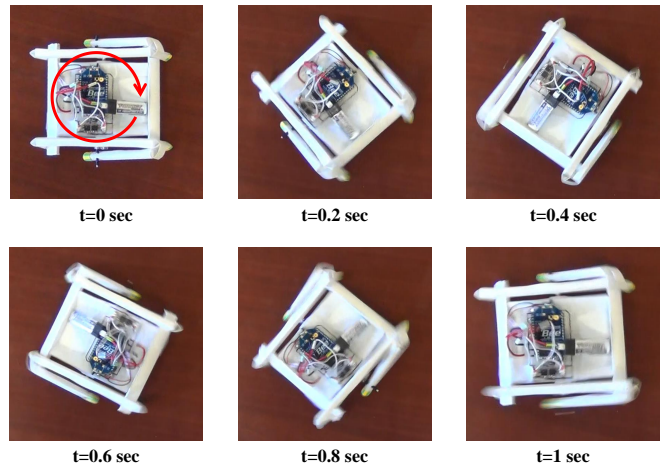


Fig. 9. Snapshots of the foldable hexapod robot prototype during an in-place turning experiment.

robot was measured at approximately 1 revolution per second or 60 rpm. Fig. 9 shows snapshots of the robot during an in-place turning experiment over an angular displacement of 360 degrees.

## V. CONCLUSION

This paper presented the design and fabrication of a 42 g foldable hexapod robot made of a sheet of polyester for swarm applications over rough terrain. The robot was 'printed' and folded in less than one hour from scratch. No external fastener such as screws or other tools are used or required during robot manufacturing. The robot has built-in polyester fasteners considered in its crease pattern. Because of the material used to fabricate the robot, it is robust against collision.

The robot was constructed from two extended four-bar

mechanisms which are connected to the sides of the main body. The robot can be adjusted for different speeds simply by controlling the speed of the motors. Two motors are used to drive the four-bar mechanisms, one for each side. The four-bar mechanisms in the crease pattern can be modified to maneuver over different obstacles with different sizes. Design flexibility, ease of fabrication, and low price make the robot suitable for swarm objectives. In this paper, the kinematics of the robot was analyzed and the four-bar mechanisms were optimized for maximum velocity. Experimental results showed that the foldable hexapod robot achieves a forward running speed of 5 body length per second and in-place turning speed of 1 revolution per second.

Future work includes overcoming the phase difference between two motors to keep the foldable hexapod robot operate at the optimal speed with minimal variation. Also, a controller needs to be designed and utilized to get accurate motions of the robot in any desired direction. After these initial steps, future work will focus on experimental swarm algorithms for collaborative control of many foldable hexapod robots on unstructured terrain. Although we ran the robot many times in different directions over various surfaces including different flooring, the robot cannot traverse over highly obstacles. The reason is that the ground clearance of the robot is only 15 mm. The next version of the robot will be considered to have larger ground clearance to overcome this shortage.

#### REFERENCES

- [1] A. T. Baisch and R. J. Wood, "Design and fabrication of the harvard ambulatory micro-robot," in *Robotics Research*, pp. 715–730, Springer, 2011.
- [2] R. Sahai, S. Avadhanula, R. Groff, E. Steltz, R. Wood, and R. S. Fearing, "Towards a 3g crawling robot through the integration of micro-robot technologies," in *IEEE International Conference on Robotics and Automation*, pp. 296–302, 2006.
- [3] A. M. Hoover, E. Steltz, and R. S. Fearing, "Roach: An autonomous 2.4 g crawling hexapod robot," in *IEEE/RSJ International Conference on Intelligent Robots and Systems*, pp. 26–33, 2008.
- [4] A. T. Baisch, C. Heimlich, M. Karpelson, and R. J. Wood, "Hamr3: An autonomous 1.7 g ambulatory robot," in *IEEE/RSJ International Conference on Intelligent Robots and Systems*, pp. 5073–5079, 2011.
- [5] A. M. Hoover and R. S. Fearing, "Fast scale prototyping for folded millirobots," in *IEEE International Conference on Robotics and Automation*, pp. 886–892, 2008.
- [6] A. T. Baisch, P. Sreetharan, and R. J. Wood, "Biologically-inspired locomotion of a 2g hexapod robot," in *IEEE/RSJ International Conference on Intelligent Robots and Systems*, pp. 5360–5365, 2010.
- [7] D. E. Soltero, B. J. Julian, C. D. Onal, and D. Rus, "A lightweight modular 12-dof print-and-fold hexapod," in *IEEE/RSJ International Conference on Intelligent Robots and Systems*, 2013.
- [8] P. Birkmeyer, K. Peterson, and R. S. Fearing, "Dash: A dynamic 16g hexapedal robot," in *IEEE/RSJ International Conference on Intelligent Robots and Systems*, pp. 2683–2689, 2009.
- [9] M. Rubenstein, C. Ahler, and R. Nagpal, "Kilobot: A low cost scalable robot system for collective behaviors," in *IEEE International Conference on Robotics and Automation*, pp. 3293–3298, 2012.
- [10] S. M. Felton, M. T. Tolley, B. Shin, C. D. Onal, E. D. Demaine, D. Rus, and R. Wood, "Self-folding with shape memory composites," *Soft Matter*, pp. 7688–7694, 2013.
- [11] S. M. Felton, M. T. Tolley, C. D. Onal, D. Rus, and R. J. Wood, "Robot self-assembly by folding: A printed inchworm robot," in *IEEE International Conference on Robotics and Automation*, pp. 277–282, 2013.
- [12] C. D. Onal, R. J. Wood, and D. Rus, "An origami-inspired approach to worm robots," *IEEE Transactions on Mechatronics*, pp. 430–438, 2012.
- [13] J. J. Craig, "Introduction to robotics: mechanics and control," 2004, Prentice Hall.